N74-14593

NASTRAN ANALYSIS OF AN AIR STORAGE PIPING SYSTEM

By Clarence P. Young, Jr., A Harper Cerringer, and Richard W. Faison
NASA Langley Research Center

SUMMARY

This paper summarizes the first Langley Research Center application of NASTRAN to a complex piping design evaluation problem. Emphasis is placed on structural modeling aspects, problems encountered in modeling and analyzing curved pipe sections, principal results, and relative merits of using NASTRAN as a piping analysis and design tool. In addition, the piping and manifolding system was analyzed with SNAP (Structural Network Analysis Program) developed by Lockheed Missiles and Space Company. The parallel SNAP study provides a basis for limited comparisons between NASTRAN and SNAP as to solution agreement and computer execution time and costs.

INTRODUCTION

The new Langley Research Center (LaRC) 4.137 MN/m^2 (600 psia) air storage facility is being constructed to effect repairs to the system that was damaged in the Langley 9- by 6-foot thermal structures tunnel manifold failure in September 1971. Because of the increased concern and emphasis at LaRC on safety in facility design, a rigorous static analysis of the piping and manifolding system design was performed within the Systems Engineering Division (SED). Since NASTRAN had been used extensively within SED for analyzing aerospace-type structures, it was decided that the piping application would provide the desired degree of rigor and at the same time exercise the applicability of NASTRAN as a piping analysis tool.

The purpose of this paper is to document the results and experience gained in applying NASTRAN to a complex pressurized piping system. Although NASTRAN was not developed as a piping analysis tool, it can be used to simulate the extensional and bending behavior of pipes which can be characterized as beams. (See, e.g., ref. 1.) The basic approach is that of a stress analysis of the given design for various static loading conditions. The calculated stresses are then compared with allowable values as obtained from references 1 to 3. These comparisons serve as a basis for evaluating structural adequacy.

SYMBOLS

A cross-sectional area of pipe, m^2 (in^2)

c	distance to outermost fiber measured from bend axis, m (in.)
$F_i(PA)$	static pressure loading
h	bend characteristic (defined by eq. (1))
I	area moment of inertia of pipe cross section, m^4 (in^4)
IPS	internal pipe size
i_n	stress intensification factor
M	bending moment
P	internal pipe pressure, N/m^2 (lbf/in^2)
R	radius of pipe bend, m (in.)
r_m	mean radius of pipe, m (in.)
T	temperature, °K (°F)
t	pipe wall thickness, m (in.)
V_w	wind velocity, m/s (mph)
x,y,z	element coordinate system
α	angle measured from bend axis of pipe to point of peak stress (see fig. 5), deg
σ_B	stress predicted by elementary beam theory, N/m^2 (lbf/in^2)

Subscripts:

y	bending about Y-axis
z	bending about Z-axis

ANALYSIS

Facility Description

The new air storage facility is depicted in figure 1. Basically, the system consists of 167 air storage bottles connected by manifolding to the main header 0.61-m-diameter (24 in.) supply line. The new main header is tied to an existing overhead line which is illustrated in the photograph of figure 2. In order to assess the total interaction loading effects between the existing line and the new lines, the existing line was modeled as well.

NASTRAN Model Characteristics

The NASTRAN model of the piping and manifolding system is illustrated in the perspective plot of figure 3. The model includes the existing overhead 0.61-m (24 in.) supply line, the new 0.61-m (24 in.) line, the new 0.20-m (8 in.) and 0.25-m (10 in.) lines, 0.15-m (6 in.) manifolds, and 0.038-m (1½ in.) distribution (goosene k) connections to storage bottles. Anchor points for the piping system are as shown in figure 3 with the gooseneck lines being fixed at the air storage bottle flanges.

Bar elements are used throughout to characterize the pipe elongation, twist, and bending behavior. In total 754 bar elements were used with the reduced problem (constraints and boundary conditions imposed) being characterized by approximately 3500 degrees of freedom.

Curved Pipe Considerations

One of the more interesting aspects of the analysis concerns the structural modeling and prediction of stresses in curved pipe sections. It is known that curved pipe sections behave quite differently compared with straight sections when subjected to bending loads. When bending loads are imposed on a curved pipe, the cross section tends to ovalize or flatten on one side, which results in increased flexibility and a stress redistribution. (See, e.g., ref. 1.)

Structural modeling and flexibility effects.- Since there are no curved bar elements within NASTRAN, the pipe elbows were modeled as a series of straight bar elements as illustrated in figure 4. For the 90° elbows in the 0.61-m (24 in.) line, three bar elements of equal length were used to complete the turn. Additionally, the pressure loadings $F_i(PA)$ shown acting in the figure were developed to satisfy equilibrium around the bend. It should be noted that the number of elements used to represent the curved pipe sections varied, depending on pipe size and turn angle. For example, the 90° bend on the 0.038-m (1½ in.) pipes was modeled using one bar element connecting the pipe center-line points of tangency.

In order to characterize the increased flexibility in the curved regions, the bending modulus of each element was reduced by a flexibility factor defined as the ratio of the resulting increased deflection of a curved pipe to that predicted by beam theory. Theoretical flexibility factor data were obtained from reference 1, which gives the flexibility factor as a function of the bend characteristic h defined as

$$h = \frac{tR}{r_m^2} \tag{1}$$

Stress intensification.- Elementary beam theory cannot account for the actual stress distributions in curved pipe as illustrated by the comparative distributions given in figure 5. Whereas beam theory would predict the maximum stress to occur at the outermost point from the bend axis, curved pipe theory shows that the peak stress shifts toward the neutral axis (corresponds

to $\alpha = 0$ in fig. 5) and also becomes intensified. The ratio of the maximum stress in a curved pipe to that predicted for a straight pipe is defined as the stress intensification factor i_n. Also, not only do the longitudinal stresses become amplified, but high circumferential stresses are predicted as well.

In figure 5, the orientation of the predicted points of maximum stress for both in-plane and out-of-plane bending of the elbow is seen to be 26° measured from the bend axes. In-plane bending is defined as a bending moment about an axis normal to the plane of bend (Z-axis in fig. 5) while out-of-plane bending corresponds to a moment about an axis in the plane of bend (Y-axis in fig. 5). The i_n values for the elbow of figure 5 as predicted by data given in references 1 and 2 are as follows:

	Reference 1	Reference 2
i_1 (circumferential)	6.6	3.5
i_2 (longitudinal).	5.0	3.5
i_3 (longitudinal).	4.3	3.5
i_4 (circumferential)	7.0	3.5

Note that values given in reference 2 are about one-half the theoretical values given in reference 1 and are constant for both in-plane and out-of-plane bending. The lower values are based largely on experimental results and appear to be more realistic for design.

It is apparent that the actual stress distributions in the curved regions become quite complex for the situation where both in-plane and out-of-plane bending loads are present. Time did not permit research into the area of stress determination around the pipe for combined bending loads; therefore, predicted maximum stresses were added in the most adverse manner as a conservative approach.

Applied Loads

The static loads used for the analysis included the total pressure, thermal loadings for a temperature rise and fall of 288° K (60° F), gravity loads, and steady wind loads at 44.7 m/s (100 mph). Solutions were obtained for the independent loading conditions as well as for the total combined loads. In this manner, the stress contributions for the separate and combined loadings were obtained for comparison with the allowable working stress criteria given in references 2 and 3.

Analysis Procedure

The analysis procedure is depicted in the flow diagram of figure 6. Note from the flow diagram the incorporation of the flexibility and stress intensification factors. As stated previously, the bending flexibility in the elbow regions was accounted for by reducing the section modulus of the bar elements which make up the curved pipe sections.

Since NASTRAN cannot recover the combined stresses for either straight or curved sections of pressurized pipe, it became necessary to write a separate stress calculations program. This program uses the input of element forces and moments and generates the combined pressurized pipe stresses (e.g., hoop stresses are accounted for along with torsional stresses) and also applies the stress intensification factors in the elbow regions. Once the combined stresses are calculated for the highest loaded elements, these values are then compared with the allowables and guideline values of references 1 to 3.

DISCUSSION OF RESULTS

The results of the NASTRAN analysis proved to be quite beneficial not only for verifying the adequacy of design but also for identifying potential problem areas and for efficient selection of anchor point locations and pipe bend radii. For example, one early finding in the analysis identified an overstressed situation for the gooseneck at the last row of air storage bottles nearest the main header. In this instance, an error in the design calculations had resulted in a pipe length selection that was too short. Had the NASTRAN analysis not been performed the error probably would have gone unnoticed with failure likely.

General Stress Results

In general the calculated stresses throughout the system were within the required working allowables of references 1 to 3 and in only a few isolated areas equaled or slightly exceeded the conservative combined loading stress guidelines given in reference 1. (The calculated stress values are not presented or discussed in detail for reasons of brevity and lack of significance within the framework of the present paper.) Based on the NASTRAN calculations, the design was acceptable; however, the design was also examined in view of obtaining stress reductions in particular areas of concern. As it turned out, the stress condition of the greatest concern occurs in the last goosenecks nearest the 0.61-m (24 in.) main header. The higher stresses occur in these goosenecks as a result of thermal and pressure expansion in the main header pipe. Two options considered for reducing these stresses were (1) to relocate the anchor point and (2) to select a more desirable bend radius for the goosenecks. These options are examined in the following subsection.

Analysis of Potential Stress Reductions

Two selected studies on stress reduction in the gooseneck pipes are discussed in this section. Other studies were made which proved to be useful for identifying local problem areas but are beyond the scope of the present paper.

Anchor point location.- The main header line and manifolding to the air storage bottles are illustrated in the schematic of figure 7. The point of fixity is located at x = 17.07 m (672 in.) (support tower) with guide locations as indicated. It should be noted that a guide support is designed to allow the pipe to slide (longitudinally) while providing constraint in all other directions.

The basic behavior which leads to the previously mentioned high stresses in the last row of distribution lines (goosenecks) is thermal and pressure expansion of the main header. The local deformation behavior of a row of goosenecks due to the main header expansion is illustrated in figure 8. The fixity at $x = 17.07$ m (672 in.) leads to pipe expansions both toward the origin $x < 17.07$ (672 in.) (negative) and toward the air storage bottle field $x > 17.07$ m (672 in.) (positive). These expansions significantly influence stresses in the gooseneck lines and in the main header elbow located at the origin. Therefore, a logical way to reduce the gooseneck stresses, at the expense of increasing the elbow stresses, would be to relocate the anchor point.

In order to examine the main header expansion behavior, the point of fixity was removed which yields the deflections along the header for pressure and temperature expansion as shown in the graph of figure 7. Note from the curves of figure 7 that a node point ($\Delta x = 0$) exists at $x = 27.94$ m (1100 in.). The node point is ideal for anchor location for the statics load problems as it would be equivalent to the no-fixity case.

In order to explore the stress situation at the particular points of concern, the anchor point locations were varied which gave the stress plots in figure 9. By combining stresses due to thermal plus temperature expansion, it can be seen that a significant stress reduction is obtained by moving the anchor point toward the bottle field. At the same time the stresses are observed to rise in the main header elbow. For example, the combined stresses in the 0.038-m (1½ in.) pipe can be reduced by 50 percent by locating the anchor at $x = 31.09$ m (1224 in.) (extrapolated point) at the expense of a 33-percent increase in the elbow. The need to have a complete fixity in view of dynamic blowdown effects and at the same time give a much reduced static stress situation would suggest locating the anchor at $x = 31.09$ m (1224 in.).

Bend radius selection for gooseneck geometry.- Another example of stress reduction via NASTRAN analysis is shown in figure 10. The 0.038-m (1½ in.) gooseneck between the 0.15-m (6 in.) manifold pipe and bottle (assumed as the point of fixity) was initially designated with a length of 0.53 m (21 in.) from manifold to bottle instead of 1.52 m (5 ft). As previously mentioned, the preliminary NASTRAN analysis resulted in unacceptably large stresses, which ultimately led to a parametric study to determine the best design. A space limitation imposed a maximum of 1.52 m (5 ft) available for the length from manifold to bottles, whereas the bottle spacing imposed a maximum radius of bend of 0.46 m (18 in.) for the 0.038-m (1½ in.) gooseneck. Intuitively, one might think that the maximum radius of bend would provide the lesser stress; however, the stresses are seen to result primarily from the displacement of the main header as previously described. This displacement imposes a large moment at the bottle connection (fixed point in fig. 10), and thus the longer the moment arm, or rather the length from manifold to bottle, the smaller the stress. Figure 10 shows the calculated stresses in the goosenecks as a function of the radius of bend for the given 1.52 m (5 ft) length from manifold to bottle. The input for the study was the displacement of the gooseneck at the manifold end for a selected bend radius of 0.20 m (8 in.). This displacement, associated with the maximum combined for both the temperature and pressure

expansion, of the main header was assumed constant and independent of bend radius. Although the data are not depicted in figure 10, the stress increases in the bend and straight section as the 1.52 m (5 ft) length from header to bottle is decreased. Also, the standard minimum radius of bend for a 0.038-m (1½ in.) pipe as specified in reference 2 is 0.19 m (7½ in.); thus, the selected gooseneck design was for a 0.19-m (7½ in.) radius of bend and a length of 1.52 m (5 ft) from manifold to bottle.

COMPARISON OF NASTRAN WITH SNAP

The parallel SNAP analysis was performed for a number of reasons. Chief among these was the need to gain further experience to provide further check-out of the SNAP "statics" program (ref. 4). Also, the SNAP analysis served as a backup solution for NASTRAN and gave a basis for comparing and/or verifying numerical results.

The NASTRAN and SNAP structural models were developed by Gerringer and Faison, respectively, so that the analyses were independent; however, the basic element representations were used for both models. It should be noted that the SNAP model did not include the new 0.20-m (8 in.) and 0.25-m (10 in.) lines shown in figure 1; however, for comparison solutions the aforementioned lines were removed from the NASTRAN model.

The parallel analysis proved to be quite useful for uncovering modeling and loads input errors. Also, the numerical results agreement was very good as one would expect.

From a computer cost point of view, SNAP was found to be much more economical for the study. Typical comparative execution times and cost per run for a combined loads case on the Control Data 6600 computer system are as follows:

	NASTRAN	SNAP
Execution time, sec.	550	120
Cost per run, dollars.	107	15

These comparisons show the NASTRAN execution time is greater by a factor of about 4.5 and costs about seven times as much as the SNAP run. These comparisons should, of course, be recognized as that for a particular static problem solution rather than a general observation. SNAP apparently attains its low execution costs through the use of a direct elimination procedure (see ref. 5) which affords substantial savings when compared with constant or variable-width band matrix, active column, or partitioning solution methods. Information distributed by the author of reference 5 points out that in run-time comparison studies no other program was found to execute as fast as SNAP; in very large problems, very substantial differences in run time (e.g., factors of 10 or more) have often been observed.

CONCULDING REMARKS

The NASTRAN application to the new LaRC piping and manifolding system supports the adequacy of design in view of applied stress criteria. The analysis defined the static behavior of a complex piping system and significantly impacted the design in several areas.

Based on the experience gained in this application, it is believed that NASTRAN can be used as a powerful tool for design evaluation of complex piping systems. However, major additional needs for NASTRAN to be used as an efficient piping analysis tool are identified as (1) development and inclusion of curved beam elements and (2) stress recovery subroutines for pressurized pipes and curved pipe sections subjected to combined bending loads.

The parallel analysis using the SNAP program gave very good agreement in numerical results. However, SNAP proved to be much more economical for this particular problem application.

REFERENCES

1. Design of Piping Systems. M. W. Kellogg Company, John Wiley and Sons, Inc., Second Edition, 1956.

2. Petroleum Refining Piping (American Standard Code for Pressure Piping), ASA B31.3-1966. The American Society of Mechanical Engineers, 1966.

3. Nuclear Power Plant Components, ASME Boiler and Pressure Vessel Code. American Society of Mechanical Engineers, July 1971.

4. Whetstone, W. D.: Structural Network Analysis Program User's Manual, Static Analysis Version V70E. LMSC-HREC D162812, December 1970.

5. Whetstone, W. D.: Computer Analysis of Large Linear Frames. Journal of the Proceedings of the American Society of Engineers, November 1969.

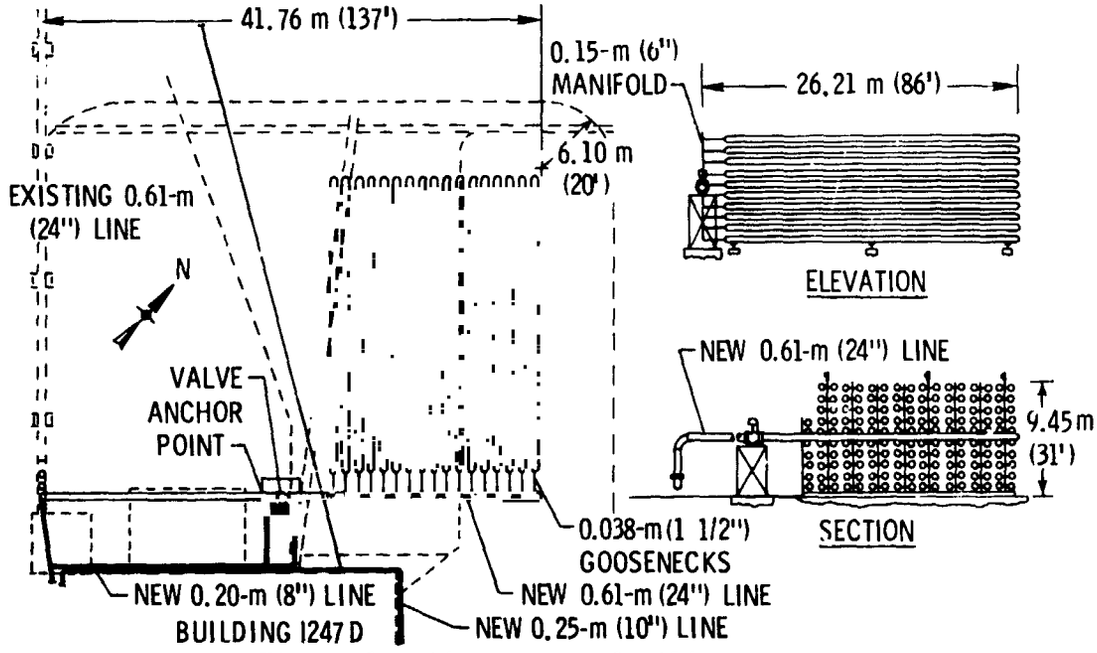

Figure 1.- Air storage facility layout.

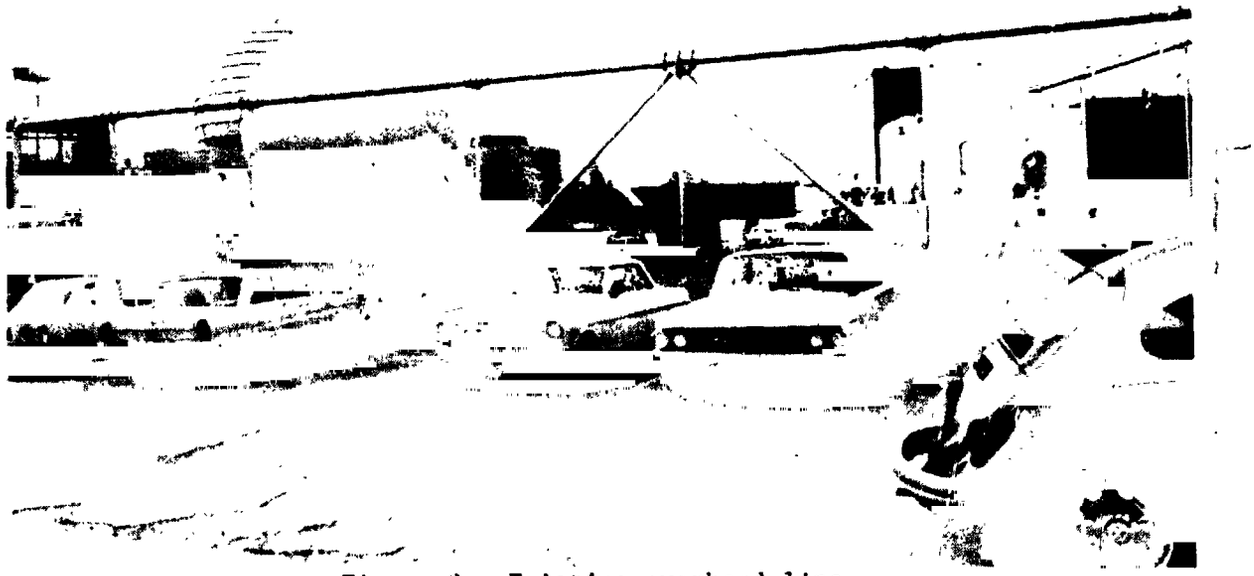

Figure 2.- Existing overhead line.

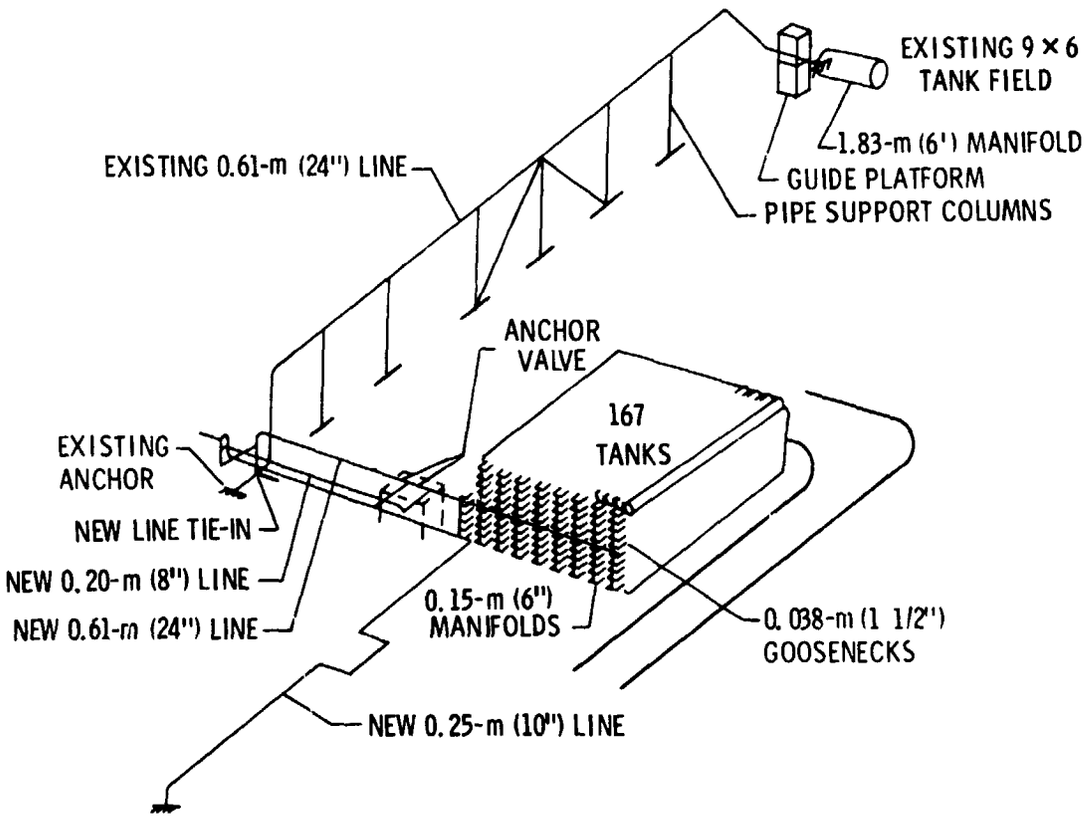

Figure 3.- Perspective of NASTRAN model.

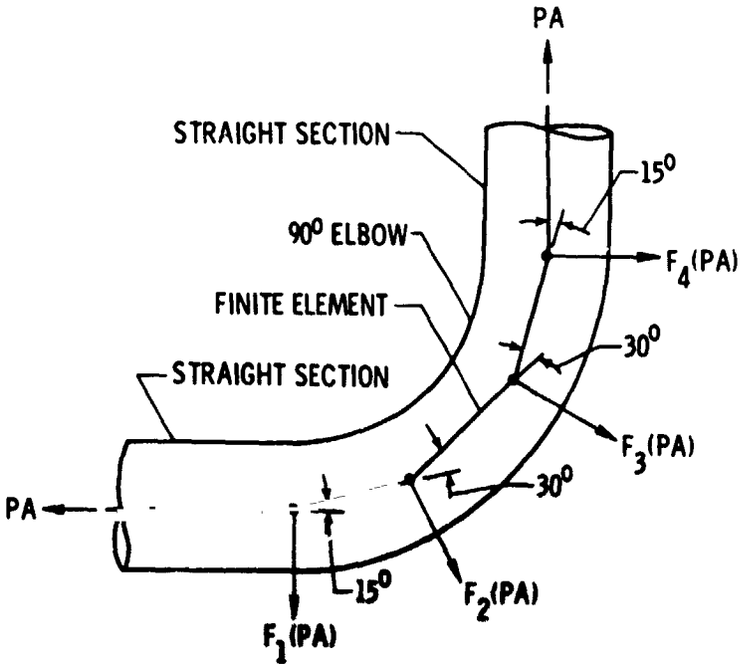

Figure 4.- Modeling of 90° pipe bend.

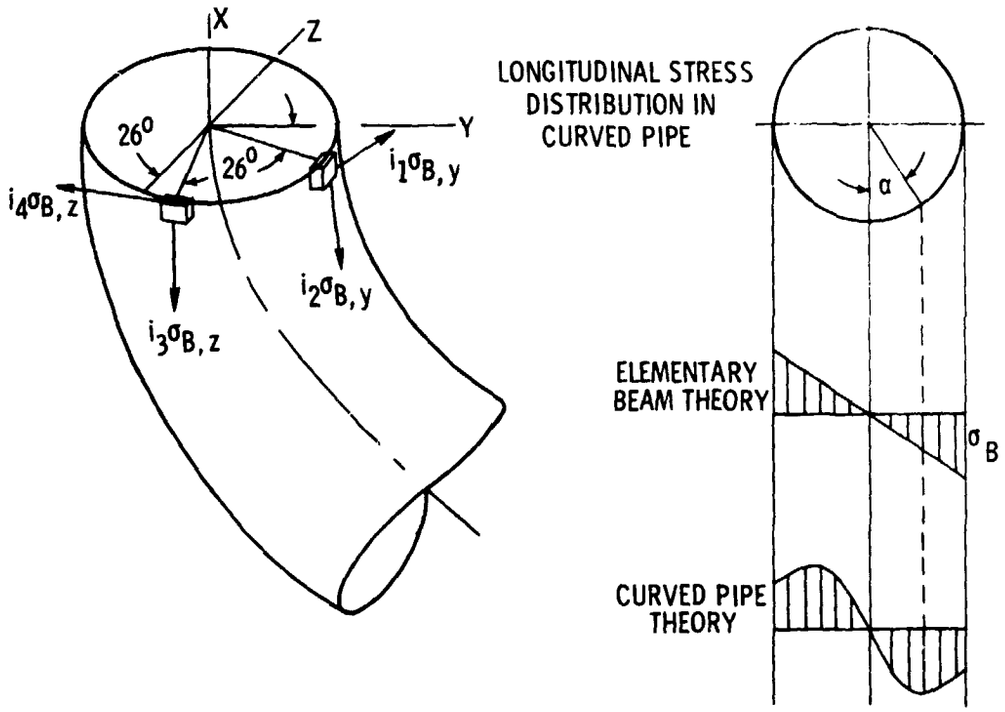

Figure 5.- Stress components for in-plane and out-of-plane bending.

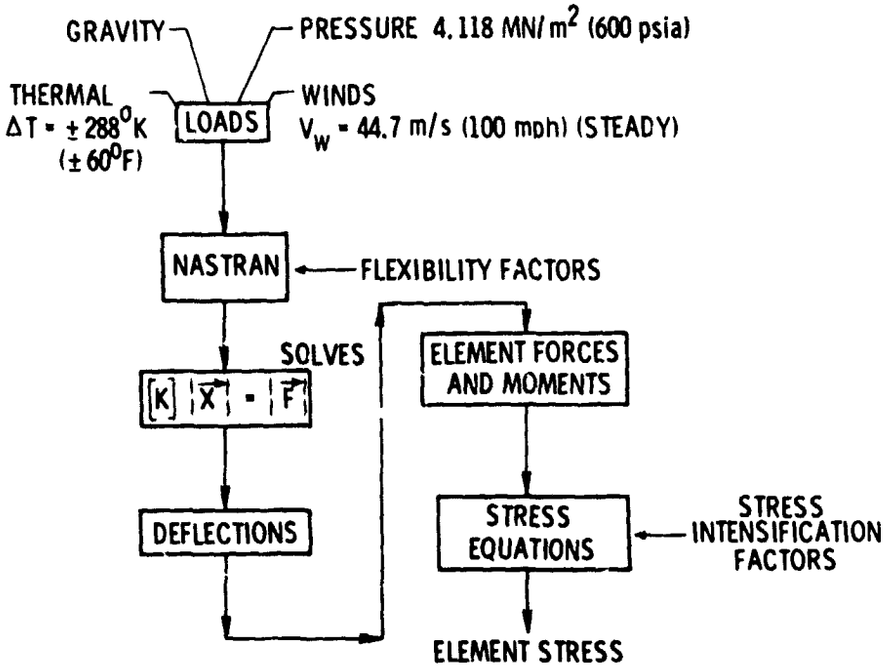

Figure 6.- Analysis procedure format.

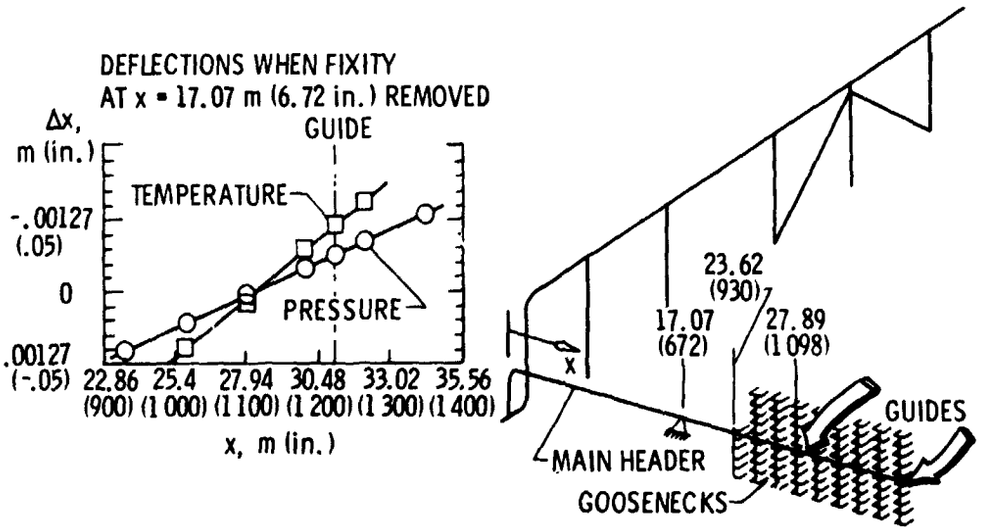

Figure 7.- The 0.61-m (24 in.) header deflections with fixity removed. Dimensions are in m (in.).

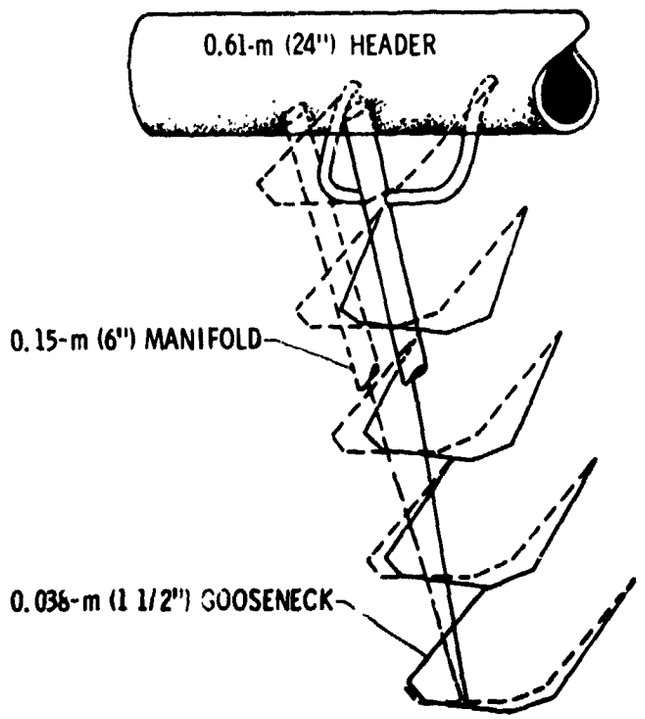

Figure 8.- Deformation behavior of goosenecks due to header movement.

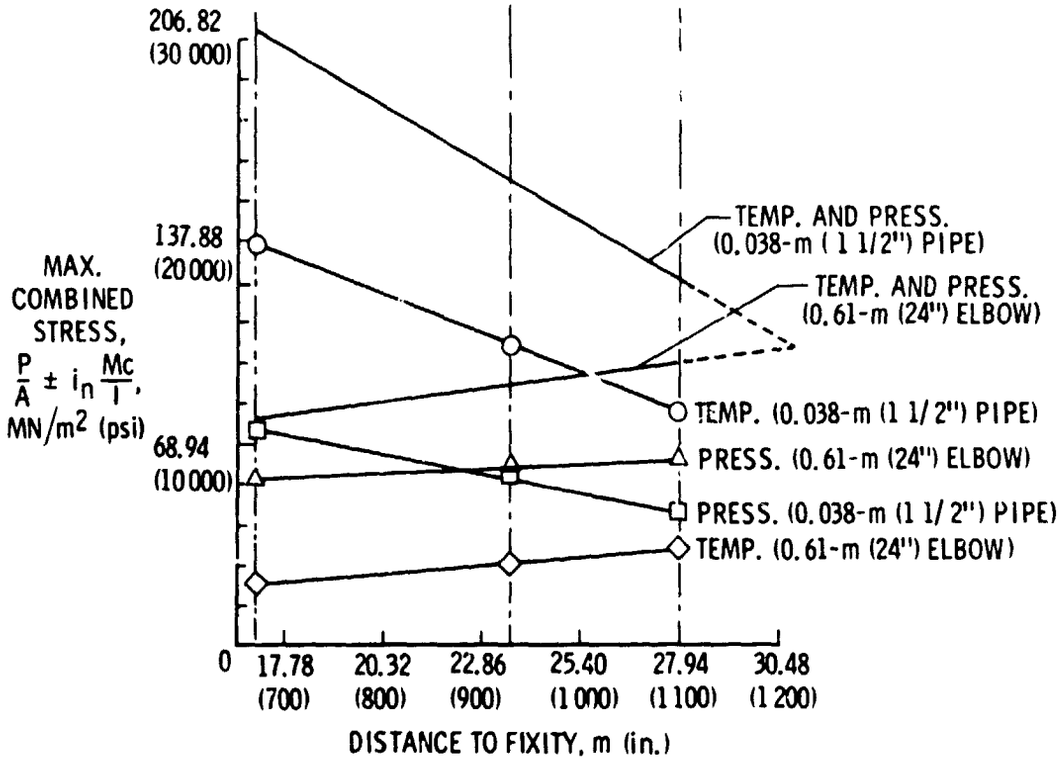

Figure 9.- Stress variations with change in anchor point location.

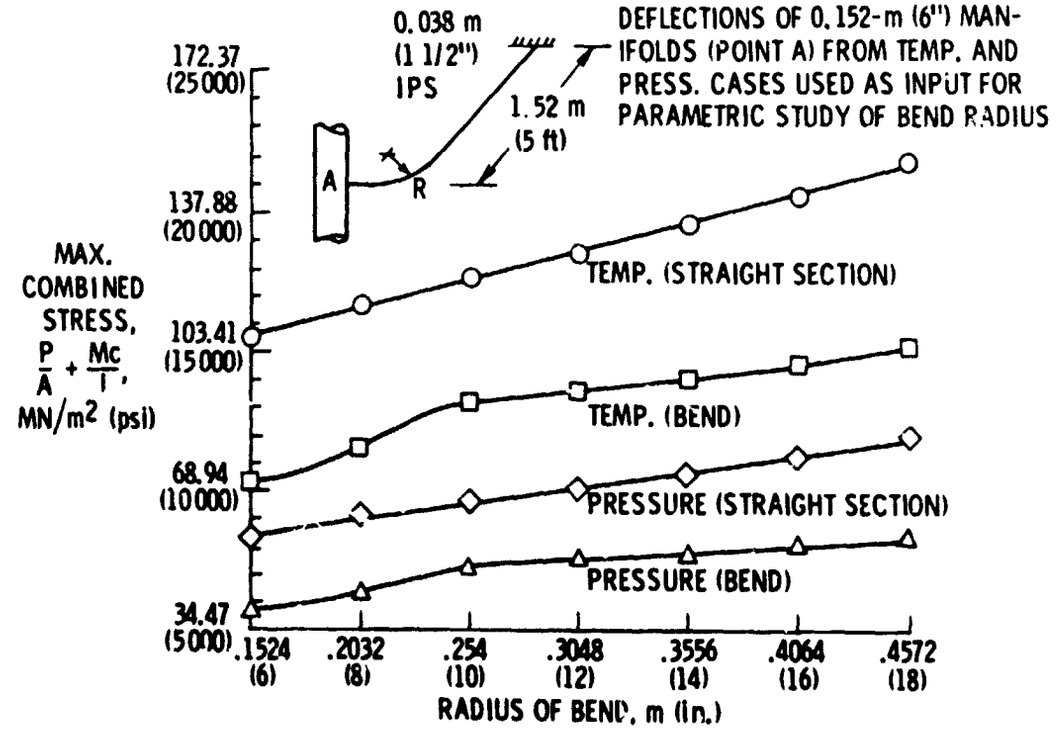

Figure 10.- Stress variations in 0.0381-m (1 1/2 in.) pipe with changes in bend radius.